

This version of the article has been accepted for publication, after peer review (when applicable) and is subject to Springer Nature's AM terms of use (<https://www.springernature.com/gp/open-research/policies/accepted-manuscript-terms>), but is not the Version of Record and does not reflect post-acceptance improvements, or any corrections. The Version of Record is available online at: <http://dx.doi.org/10.1007/s11705-021-2044-z>.

1  
2  
3  
4 **Energy-efficient recovery of tetrahydrofuran and ethyl**  
5 **acetate by triple-column extractive distillation: Entrainer**  
6 **design and process optimization**

7 Ao Yang<sup>1,2</sup>, Yang Su<sup>3</sup>, Tao Shi<sup>2</sup>, Jingzheng Ren<sup>2</sup>, Weifeng Shen(✉)<sup>1</sup>, Teng Zhou(✉)<sup>4,5</sup>

8 1 School of Chemistry and Chemical Engineering, Chongqing University, Chongqing, PR China

9 2 Department of Industrial and Systems Engineering, The Hong Kong Polytechnic University, Hong Kong  
10 Special Administrative Region, PR China

11 3 School of Intelligent Technology and Engineering, Chongqing University of Science & Technology, Chongqing  
12 401331, PR China

13 4 Process Systems Engineering, Otto-von-Guericke University Magdeburg, D-39106 Magdeburg, Germany

14 5 Process Systems Engineering, Max Planck Institute for Dynamics of Complex Technical Systems, D-39106  
15 Magdeburg, Germany

16 © Higher Education Press and Springer-Verlag GmbH Germany 2017

17 Received Nov 08, 2020; accepted MM DD, 2021

18 E-mail: shenweifeng@cqu.edu.cn and zhout@mpi-magdeburg.mpg.de

19 **Abstract** An energy-efficient triple-column extractive distillation process is developed for recovering  
20 tetrahydrofuran and ethyl acetate from industrial effluent. The process development follows a rigorous  
21 hierarchical design procedure that involves entrainer design, thermodynamic analysis, process design and  
22 optimization, and heat integration. The computer-aided molecular design method is firstly used to find promising  
23 entrainer candidates and the best one is determined via rigorous thermodynamic analysis. Subsequently, the direct  
24 and indirect triple-column extractive distillation processes are proposed in the conceptual design step. These two  
25 triple-column extractive distillation processes are then optimized by employing an improved genetic algorithm.  
26 Finally, heat integration is performed to further reduce the process energy consumption. The results indicate that  
27 the indirect triple-column extractive distillation process with heat integration shows the highest performance in  
28 terms of the process economics.

29 **Keywords** extractive distillation, solvent selection, conceptual design, process optimization, heat integration

30 **1 Introduction**

31 Tetrahydrofuran (THF) and ethyl acetate (EtAC) are regularly used as organic solvents and biofuels as well as  
32 sustainable biomass energy sources for the internal combustion engines [1-2]. According to the report from He  
33 et al. [3], wastewater mixtures containing THF and EtAC are generally produced in the chemical and  
34 pharmaceutical industries. However, the separation of such mixtures is difficult via the conventional distillation  
35 process because the distillation boundary and multiple azeotropes exist in this system. Thereby, the explorations  
36 of efficient processes for separating such mixtures are significant in realizing the recovery of available resources  
37 and reducing the environmental pollution [4-5].

38 Extractive distillation (ED) [6-7], pressure-swing distillation [8-9] and azeotropic distillation [10-11] are  
39 employed as effective approaches to separate azeotropic mixtures. Pressure-swing distillation is limited to

40 pressure-sensitive systems [12] and multiple steady-states can exist in the azeotropic distillation process [13].  
41 Therefore, the ED process becomes one of the most popular separation techniques for handling azeotropic or  
42 close-boiling systems in the chemical and petroleum industries due to its advantage in the operational and control  
43 aspects [14-15]. For example, Yang et al. [16] reported an ED process to separate the binary azeotropic mixture  
44 dimethyl carbonate and ethanol by varying the operating pressures. Shi et al. [17] explored the separation of the  
45 ternary mixture isopropyl alcohol/isopropyl acetate/water with multiple azeotropes via two-alternative ED  
46 schemes. The separation of azeotropic systems has also been investigated by other researchers [18-20] using ED.

47 The selection of entrainer plays a key role in designing the energy-saving ED processes [21-22]. Cui et al.  
48 [23] studied the separation performance of two different entrainers via phase diagram analysis and they found  
49 that ethylene glycol is more suitable for the separation of benzene/isopropanol/water by ED. Zhu et al. [24]  
50 developed a heuristic method employing the relative volatility to determine the optimal solvent with the best  
51 economic performance. Shen et al. [25] proposed a solvent selection approach employing five properties (i.e.,  
52 relative volatility, solubility power, molecular weight, melting point and boiling point) as objectives to screen the  
53 best entrainer. Blahušiak et al. [26] developed another quick calculation procedure for the preselection of solvents  
54 by considering the minimum energy consumption and solvent-to-feed ratio. The efficiency and reliability of this  
55 method were successfully verified via several industrial application cases. Unfortunately, these previous works  
56 all considered a limited, pre-specified solvents and tried to find the best candidate from these solvents. In  
57 comparison with the previous solvent screening methods, the computer-aided molecular design (CAMD) method  
58 developed by Gani and Brignole [27] attempts to rationally design the most suitable solvents [28-33] from a list  
59 of molecular building groups. Recently, Zhou et al. [34] proposed a multi-objective CAMD approach to design  
60 solvents for the separation of binary azeotropic mixture *n*-hexane/methanol. In the present work, we use this  
61 method to find potential entrainers for the ternary azeotropic system THF/EtAC/water. Subsequently,  
62 thermodynamic insights are employed to further determine the best entrainer for the ED process.

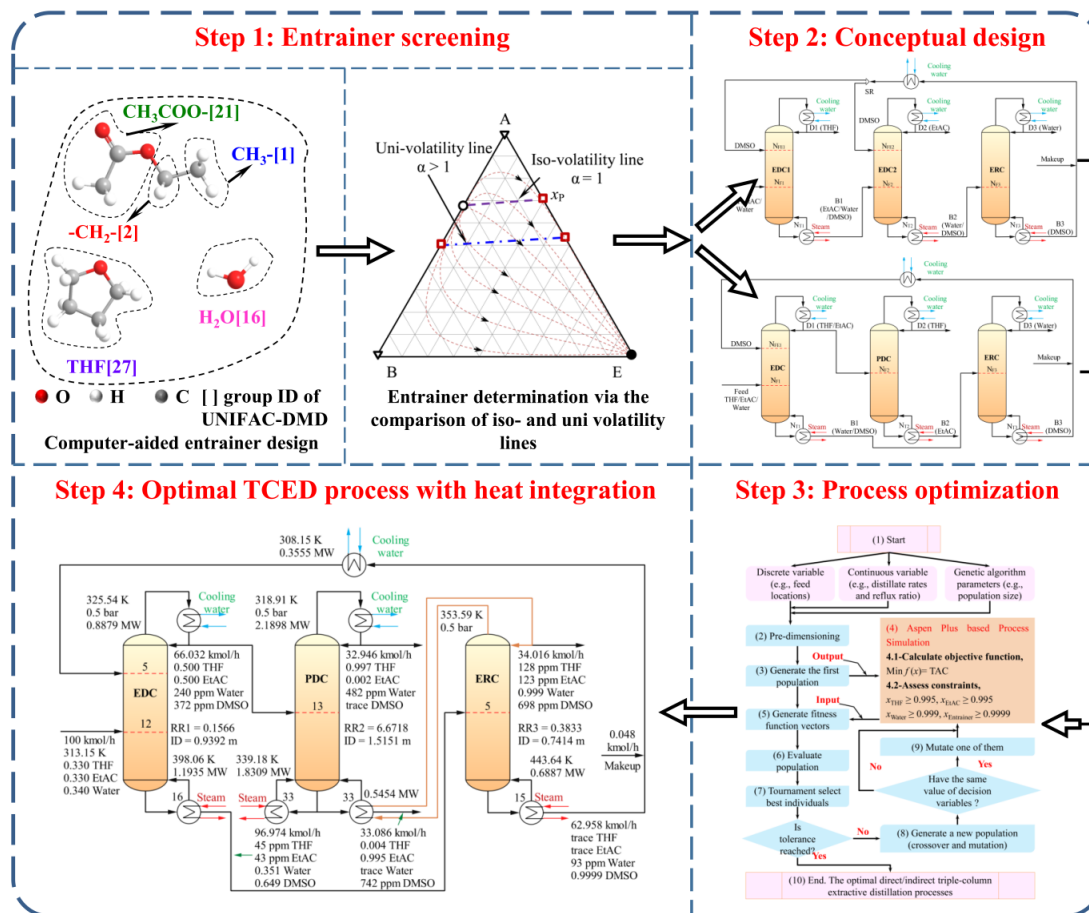
63 In addition to the optimal selection of solvent, energy saving could be further achieved by the process  
64 optimization technique [35]. Waltermann et al. [36] formulated extractive and heteroazeotropic distillation  
65 process design tasks into mixed-integer nonlinear programming (MINLP) problems and solved them as a series  
66 of successively relaxed nonlinear programming problems. Krone et al. [37] proposed a superstructure-based  
67 modeling environment to facilitate the MINLP optimization of complex distillation processes where rigorous  
68 thermodynamic models are used. It should be noted that conventional gradient-based optimization algorithms are  
69 not efficient for handling complex MINLP problems in distillation processes with massive coupled discrete and  
70 continuous decision variables [38]. By contrast, stochastic or hybrid optimization algorithms can be very  
71 powerful for solving these problems [39]. For example, Kruber et al. [40] optimized ED processes using a hybrid  
72 evolutionary-deterministic optimization approach. Yang et al. [41] optimized a thermally coupled ED process via  
73 the genetic algorithm (GA). You et al. [42] discussed the optimization of the ED process by using the SQP and  
74 GA approaches and they proved that the process economic performance can be further improved via the GA-  
75 based optimization.

76 In this work, we develop an efficient extractive distillation process to recover THF and EtAC from industrial  
77 wastewater. A rigorous hierarchical design procedure involving entrainer design, thermodynamic analysis,  
78 process design and optimization, and heat integration (HI) is followed in the process development. Specifically,  
79 candidate entrainers for the separation of THF/EtAC/water are first screened via the CAMD method. The iso-  
80 and uni- volatility lines between the azeotropic mixture and the entrainer are compared to obtain the most efficient  
81 entrainer for the separation task. Subsequently, volatility orders and distillation sequences (i.e., direct and indirect  
82 separation flowsheets) are determined in the conceptual design step. An improved GA is then employed to  
83 optimize the direct and indirect ED processes. Finally, HI is performed to further reduce the energy consumption  
84 of the processes.

## 85 2 Methodology

86 A systematic approach (as illustrated in Fig. 1) involving the selection of entrainer via CAMD and  
87 thermodynamic analysis, conceptual design, process optimization, and HI is proposed to find an energy-efficient  
88 ED process for the separation of the ternary azeotropic mixture THF/EtAC/water. In Step 1, candidate entrainers  
89 are first designed via the CAMD method and then the most suitable entrainer is determined via the comparison

90 of iso- and uni- volatility lines of the ternary phase diagrams. In Step 2, the conceptual design of the ED process  
 91 considering the direct and indirect separation sequences is performed via the rigorous thermodynamic analysis.  
 92 In Step 3, an improved GA is used to optimize the operating variables (e.g., total number of stages and reflux  
 93 ratios) for both direct and indirect separation processes. Finally, in Step 4, HI is performed for the optimized  
 94 processes to further reduce the energy consumptions.



95  
 96 **Fig. 1** Systematic approach for conceptual design and optimization of the THF/EtAC/water separation process

## 97 2.1 Screening of entrainer

### 98 2.1.1 Computer-aided entrainer design

99 The entrainer plays a significant role in the ED process [43]. In this work, the CAMD approach is employed to  
 100 obtain the potential candidate entrainers. In total, 22 UNIFAC-Dortmund (UNIFAC-DMD) groups for building  
 101 the entrainer molecules are considered in this work. Their UNIFAC-DMD group IDs, valences, and maximum  
 102 occurrences are listed in Table 1. The van der Waals volume  $R_j$  and surface area  $Q_j$  are summarized in Table S1.

103 **Table 1** Functional groups and single-group molecules with their IDs, valences, and maximum numbers

Group ID	Group $j$	Valence $v(j)$	Group classification
1	CH <sub>3</sub>	1	Mg <sup>a</sup>
2	CH <sub>2</sub>	2	Mg <sup>a</sup>
3	CH	3	Mg <sup>a</sup>
4	C	4	Mg <sup>a</sup>
14	OH(P)	1	Ceg <sup>b</sup>

Group ID	Group $j$	Valence $v(j)$	Group classification
15	CH <sub>3</sub> OH	0	Sg <sup>e</sup> )
16	H <sub>2</sub> O	0	Sg <sup>e</sup> )
18	CH <sub>3</sub> CO	1	Ceg <sup>b</sup> )
19	CH <sub>2</sub> CO	2	Nceg <sup>d</sup> )
20	CHO	1	Ceg <sup>b</sup> )
21	CH <sub>3</sub> COO	1	Ceg <sup>b</sup> )
22	CH <sub>2</sub> COO	2	Nceg <sup>d</sup> )
23	HCOO	1	Ceg <sup>b</sup> )
24	CH <sub>3</sub> -O	1	Ceg <sup>b</sup> )
25	CH <sub>2</sub> -O	2	Nceg <sup>d</sup> )
26	CH-O	3	Nceg <sup>d</sup> )
27	THF	0	Sg <sup>e</sup> )
61	Furfural	0	Sg <sup>e</sup> )
67	DMSO	0	Sg <sup>e</sup> )
72	DMF	0	Sg <sup>e</sup> )
81	OH(S)	1	Ceg <sup>b</sup> )
82	OH(T)	1	Ceg <sup>b</sup> )

104 a) Mg: main groups; b) Ceg: chain-ending function groups; c) Sg: single-group molecules; d) Nceg: non chain-ending  
105 function groups.

106 Following the study of Zhou et al. [34], the solvent infinite dilution selectivity ( $S_{AB}^{\infty}$ ) and infinite dilution  
107 capacity toward B ( $C_B^{\infty}$ ) as shown in Eqs. 1-2 can be used in the CAMD program to find promising entrainers  
108 for the separation of B from A using ED. Herein, due to the trade-off between these two selection criteria, we  
109 introduced a weighted function, displayed in Eq. 3, as our final objective function.

$$S_{AB}^{\infty} = \frac{\gamma_A^{\infty}}{\gamma_B^{\infty}} \quad (1)$$

$$C_B^{\infty} = \frac{1}{\gamma_B^{\infty}} \quad (2)$$

$$\text{Objective function} = \max(\omega_1 S_{AB}^{\infty} + (1 - \omega_1) C_B^{\infty}) \quad (3)$$

110 where  $\omega_1$  and  $(1 - \omega_1)$  represent the weight coefficients of  $S_{AB}^{\infty}$  and  $C_B^{\infty}$ , respectively. In the CAMD  
111 approach,  $\omega_1$  is a variable from 0.0 to 1.0 with a step size of 0.1.  $\gamma_A^{\infty}$  and  $\gamma_B^{\infty}$  are the infinite dilution activity  
112 coefficients of A and B in the entrainer, respectively. They can be calculated using the UNIFAC-DMD model at  
113 the infinite dilution condition. In this work, the ternary mixture being separated has two azeotropes, THF/water  
114 and EtAC/water. Thereby, A and B indicate the THF (or EtAC) and water, respectively.

115 The molecular structure should be constrained in the CAMD to ensure that the generated molecule is  
116 structurally feasible and uncomplicated. The structural feasibility and complexity rules are taken directly from  
117 Zhou et al. [34]. The upper limit of the number of groups in the solvent molecule is set to 6. Melting and boiling  
118 points are used as the property constraints. The melting point as shown in Eq. 4 is used to ensure that the designed

119 molecules are liquid at room temperature. In the ED process, the entrainer is recovered via distillation. Thereby,  
 120 lower and upper bounds (Eq. 5) are employed to constrain the normal boiling point of the entrainer.

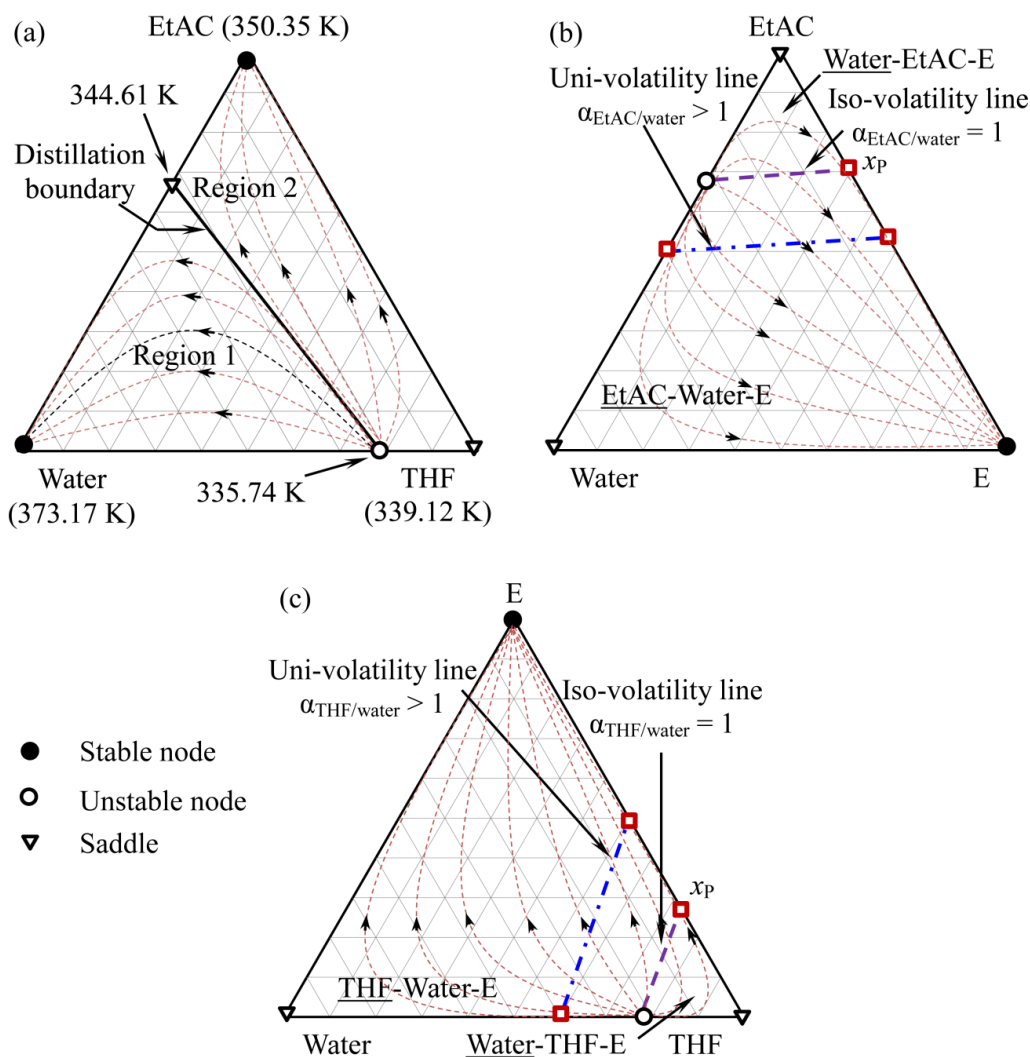
$$\sum_{j=1}^N n_j t_{m,j} \leq \exp\left(\frac{T_m^{\text{upper}}}{T_{m0}}\right) \quad (4)$$

$$\exp\left(\frac{T_b^{\text{lower}}}{T_{b0}}\right) \leq \sum_{j=1}^N n_j t_{b,j} \leq \exp\left(\frac{T_b^{\text{upper}}}{T_{b0}}\right) \quad (5)$$

121 where  $n_j$  is the number of group  $j$  present in the entrainer molecule and  $N$  denotes the total number of groups  
 122 considered in this work ( $N = 22$ , see Table 1). The upper temperature of the melting point ( $T_m^{\text{upper}}$ ) is 315 K; the  
 123 lower and upper bounds of the boiling point ( $T_b^{\text{lower}}$  and  $T_b^{\text{upper}}$ ) are 393.15 K and 493.15 K;  $T_{m0}$  and  $T_{b0}$  are  
 124 147.45 K and 222.54 K, respectively. Group contributions  $t_{m,j}$  and  $t_{b,j}$  can be found from Marrero and Gani [44].  
 125 The detailed formulation of the CAMD problem can be found in Zhou et al. [34]. The resulting mixed-integer  
 126 optimization problem is coded and solved in Python.

### 127 2.1.2 Solvent determination via the thermodynamic analysis

128 The suitable entrainer of the ED process could be further determined via the thermodynamic feasibility analysis.  
 129 Fig. 2 illustrates the residue curve maps (RCMs) of the EtAC/THF/water, EtAC/water/E and THF/water/E  
 130 systems where E indicates an arbitrary effective entrainer. As shown in Fig. 2a, there are two azeotropes (one  
 131 between THF and water and the other between EtAC and water). Their azeotropic temperatures are 335.74 K and  
 132 344.61 K and the corresponding azeotropic compositions are 78.72 mol% and 61.32 mol%, respectively. The  
 133 black dot, hollow triangle and hollow circle represent the stable node, saddle and unstable node, respectively. In  
 134 Fig. 2a, the ternary diagram is divided into two regions via the distillation boundary between azeotropes of  
 135 EtAC/water and THF/water. In Regions 1 and 2, all residue curves are directed from an unstable node to a stable  
 136 node. Due to the existence of distillation boundary, it is impossible to separate the components by simple  
 137 distillation. Fig. 2b and 2c show the RCMs with an effective entrainer. In Fig. 2b, the intersection of the iso-  
 138 volatility line and the EtAC-E edge is denoted as  $x_p$ . The position of  $x_p$  can be adopted to preliminarily evaluate  
 139 the separation performance of the entrainer E. When a heaviest entrainer has a much stronger interaction with  
 140 water (making EtAC the lightest component), the  $x_p$  point will be closer to the EtAC vertex, leading to a higher  
 141 separation performance [45]. Additionally, the performance of the entrainer can be further verified via the  
 142 intersection of the uni-volatility line and the EtAC-E edge. Water-EtAC-E indicates that water as a heavier  
 143 component (in comparison with EtAC) can be distilled out from the top of the ED column (EDC) when the total  
 144 feed composition locates above the iso-volatility line. On the other hand, when the total feed composition is  
 145 below the iso-volatility line, EtAC can be first distilled out. The analysis of the THF/water/E system in Fig. 2c is  
 146 very similar to that of the EtAC/water/E system.



147  
 148 **Fig. 2** RCMs of the (a) studied EtAC/THF/water system, (b) mixture of EtAC-water together with an entrainer E, and (c) THF-  
 149 water with an entrainer E

150 **2.2 Conceptual design via RCMs**

151 The ED process flowsheets can be designed via the analysis of the RCMs after the entrainer is determined.  
 152 Normally, we can obtain two different process flowsheets with one following the direct separation sequence and  
 153 the other following the indirect separation sequence.

154 **2.3 Process optimization**

155 The optimization of the ED process is carried out via the combination of the improved GA and Aspen Plus-based  
 156 process simulation. Fig. S1 demonstrates the scheme of the optimization process. Firstly, the discrete variables  
 157 (e.g., feed locations), continuous variables (e.g., distillate rates and reflux ratios), and GA parameters (e.g.,  
 158 population size) are imported into an improved GA based software developed in our group. The first population  
 159 is generated and sent to Aspen Plus to calculate the objective function and assess the constraints. In addition, the  
 160 results are fed back to generate fitness function vectors, evaluate population and select the best individuals. The  
 161 process optimization is terminated when the tolerance (difference between adjacent objective function values)  
 162 satisfies the stop criteria. Otherwise, a new generation is created. The created generation is directly fed to Aspen  
 163 Plus when there is no same individual in this generation; if not, mutation is imposed on one of them.

### 164 2.3.1 Objective function

165 In this work, the total annual cost (TAC) as illustrated in Eq. 6 is used to assess the economic performance of the  
166 proposed processes, which involves two parts: total capital cost (TCC) and annual operating cost (AOC) [46].  
167 The AOC is made up of the steam and cooling water costs while the TCC includes the heat exchanger and  
168 distillation column costs. The payback period is assumed to be three years [47]. The detailed calculation of TCC  
169 and AOC could be found in the *Supporting Information*.

$$TAC = \frac{TCC}{\text{Payback period}} + AOC \quad (6)$$

### 170 2.3.2 Constraints

171 In this work, three product purities and the entrainer purity in Eq. 7 are specified as constraints for the GA-based  
172 optimization.

$$\begin{aligned} x_{\text{THF}} &\geq 99.50 \text{ mol\%} \\ x_{\text{EtAC}} &\geq 99.50 \text{ mol\%} \\ x_{\text{Water}} &\geq 99.90 \text{ mol\%} \\ x_{\text{Entrainer}} &\geq 99.99 \text{ mol\%} \end{aligned} \quad (7)$$

### 173 2.3.3 Upper and lower bounds of decision variables

174 In the optimization process, upper and lower bounds of the discrete and continuous decision variables for the  
175 direct and indirect triple-column ED (TCED) processes are summarized in Table S2. There are eight integer  
176 decision variables including the total number of stages of the three columns ( $N_{T1}$ ,  $N_{T2}$  and  $N_{T3}$ ), feed locations of  
177 entrainers ( $N_{FE1}$  and  $N_{FE2}$ ) and feed locations of the three columns ( $N_{F1}$ ,  $N_{F2}$  and  $N_{F3}$ ). Continuous decision  
178 variables include molar reflux ratios ( $RR_1$ ,  $RR_2$  and  $RR_3$ ), flow rate of entrainer ( $F_E$ ), split ratio of entrainer (SR),  
179 and distillate rates ( $D_1$ ,  $D_2$  and  $D_3$ ).

## 180 2.4 HI

181 The HI technique could be employed to reduce the process energy consumption when a sufficient temperature  
182 difference exists between the condenser and the reboiler [48].

# 183 3 Results and discussion

## 184 3.1 The entrainer screening

### 185 3.1.1 Results of CAMD

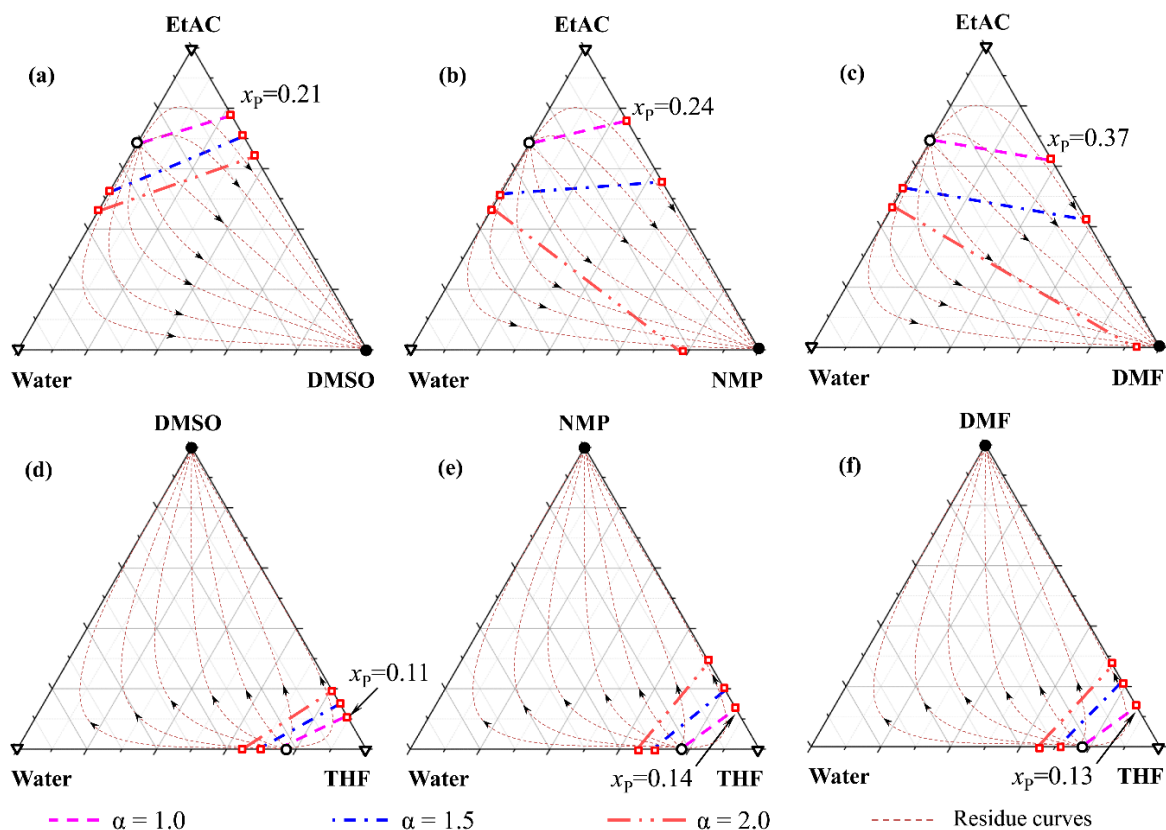
186 There are two binary azeotropes EtAC/water and THF/water in the ternary mixture EtAC/THF/water. In the  
187 UNIFAC-DMD model, EtAC is divided into three groups, CH<sub>3</sub>, CH<sub>2</sub>, and CH<sub>3</sub>COO, and THF and water are  
188 single-group molecules. After the CAMD computation, dimethyl sulfoxide (DMSO), furfural and N,N-  
189 dimethylformamide (DMF) are identified as the most promising entrainers for all the different  $w_1$  values (see  
190 Table S3). According to the vapor-liquid equilibrium in Yang et al. [49], N-methyl-2-pyrrolidone (NMP) is an  
191 efficient solvent for separating the ternary mixture. Therefore, together with DMSO, DMF and furfural, NMP is  
192 considered as the fourth candidate entrainer to further verify the performance of the entrainers obtained from the  
193 CAMD.

### 194 3.1.2 Final determination of entrainer

195 The thermodynamic analyses such as iso- and uni- volatility lines are adopted to further determine the most  
196 powerful entrainer for the separation of the ternary azeotropic mixture EtAC/THF/water. The selection of  
197 thermodynamic model is important to accurately describe the vapor-liquid equilibrium of the system at different

198 temperatures. Herein, the activity coefficient model UNIQUAC is employed and the corresponding binary  
 199 interaction parameters are summarized in Table S4 (*Supporting Information*). Among the four entrainers, furfural  
 200 is first excluded because it can form an extra azeotrope with water, leading to two separate distillation regions  
 201 and thus making it incapable to separate THF/EtAC/water. For the other three entrainers, we performed a rigorous  
 202 thermodynamic analysis, as discussed below.

203 Fig. 3 displays the iso- and uni- volatility lines for azeotropes EtAC-water and THF-water using DMSO,  
 204 NMP and DMF as the entrainers. These plots are generated via the separation module ‘Flash2’ in Aspen Plus. As  
 205 demonstrated, the entrainer DMSO shows a higher performance for the separation of EtAC/water and THF/water  
 206 because its  $x_p$  point is closer to the components EtAC and THF, compared to the cases where NMP and DMF are  
 207 used. Therefore, DMSO is finally selected as our entrainer for further process design and evaluation.  
 208



209  
 210 **Fig. 3** The iso- and uni- volatility lines for (a-c) EtAC-water and (d-f) THF-water azeotropic mixtures by using the entrainers  
 211 DMSO, NMP and DMF

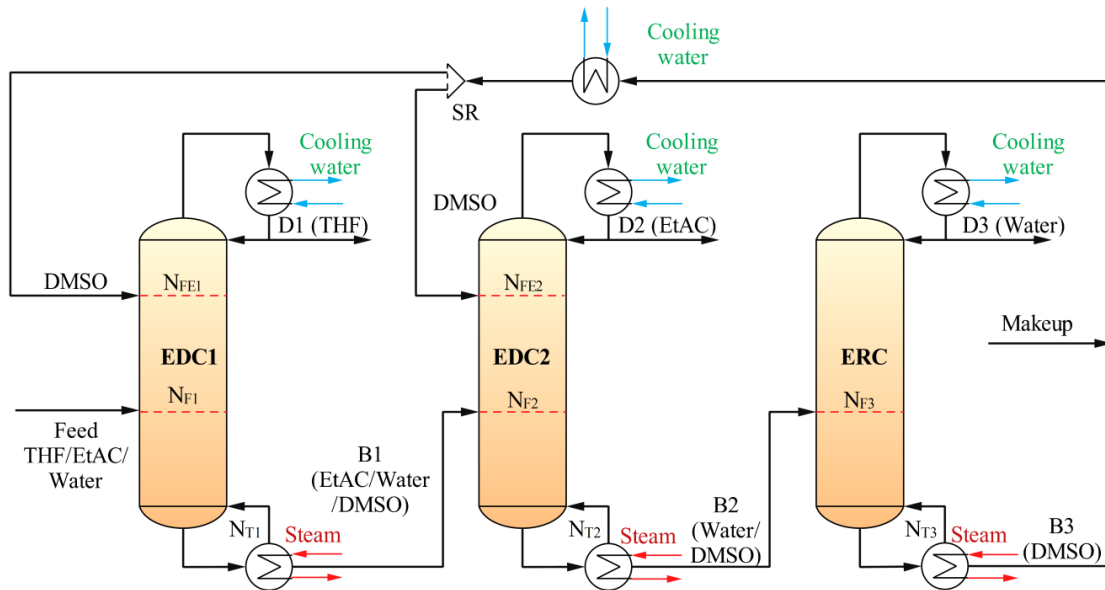
## 212 3.2 Conceptual design of the ED process

213 As seen in Fig. 3a and 3c, the point of  $x_p$  locates on the edges of EtAC-DMSO and THF-DMSO indicating that  
 214 EtAC and THF are more volatile than water when using DMSO as the entrainer. Thereby, the component THF  
 215 with the lowest boiling point can be firstly distilled out in an EDC when applying the direct separation sequence.  
 216 Subsequently, EtAC can be obtained in another EDC and finally, water and DMSO can be separated in a  
 217 conventional distillation column. In the indirect ED process, the mixture of THF and EtAC can be firstly obtained  
 218 in an EDC and then separated in another distillation column. In summary, the separation of the ternary mixture  
 219 THF/EtAC/water with two azeotropes can be achieved using DMSO as the entrainer via both the direct and  
 220 indirect separation schemes.

### 221 3.2.1 Direct separation sequence



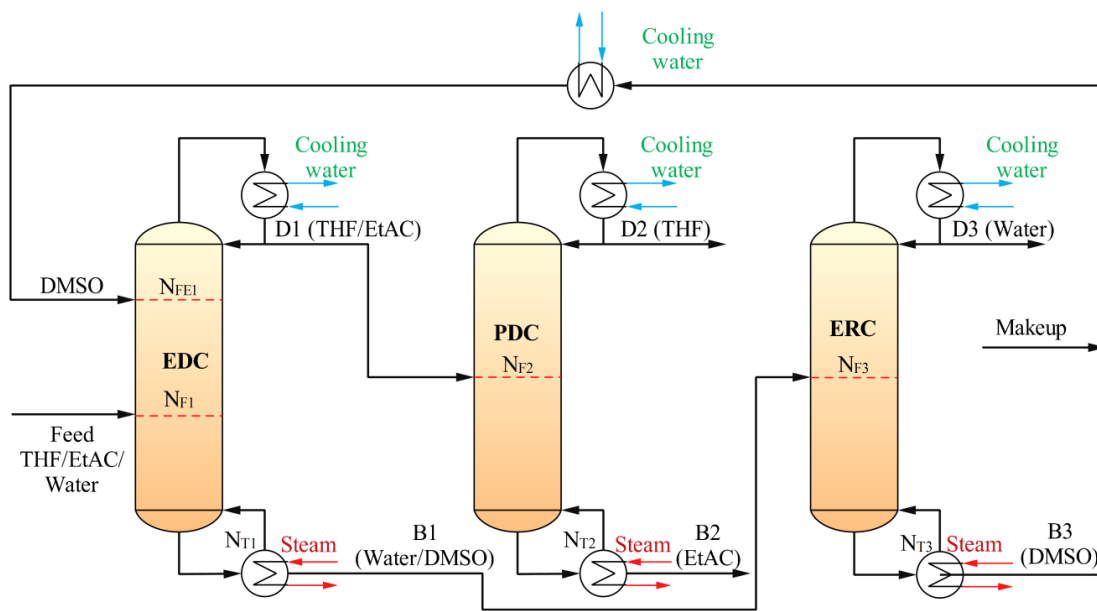
222 Fig. 4 shows the direct TCED process for separating the ternary mixture THF/EtAC/water with two azeotropes.  
 223 The process includes two EDCs (EDC1 and EDC2) and one entrainer recovery column (ERC). The entrainer  
 224 DMSO is split into two substreams. One substream and the ternary mixture THF/EtAC/water are fed into EDC1  
 225 where THF and the mixture of EtAC/water/DMSO are distilled at the top and bottom, respectively. The mixture  
 226 of EtAC/water/DMSO and the other entrainer substream are sent to EDC2 where EtAC and water/DMSO are  
 227 obtained at the top and bottom, respectively. Finally, water and DMSO are separated in the ERC. SR denotes the  
 228 ratio of the molar flow rate of the entrainer sent to EDC2 to the molar flow rate of the entire DMSO stream.



229  
 230 **Fig. 4** The scheme of the direct TCED process for separating THF/EtAC/water

### 231 3.2.2 Indirect separation sequence

232 The indirect TCED process includes one EDC, one product distillation column (PDC) and one ERC (see Fig. 5).  
 233 DMSO and the THF/EtAC/water mixture are fed into the EDC and then the mixtures of THF/EtAC and  
 234 water/DMSO are obtained at the top and bottom of the EDC, respectively. The mixture of THF/EtAC enters the  
 235 PDC and high purities of THF and EtAC are obtained at the top and bottom of PDC, respectively. The entrainer  
 236 DMSO is finally separated from water in ERC and recycled back to EDC.



237

238 **Fig. 5** The scheme of the indirect TCED process for separating THF/EtAC/water

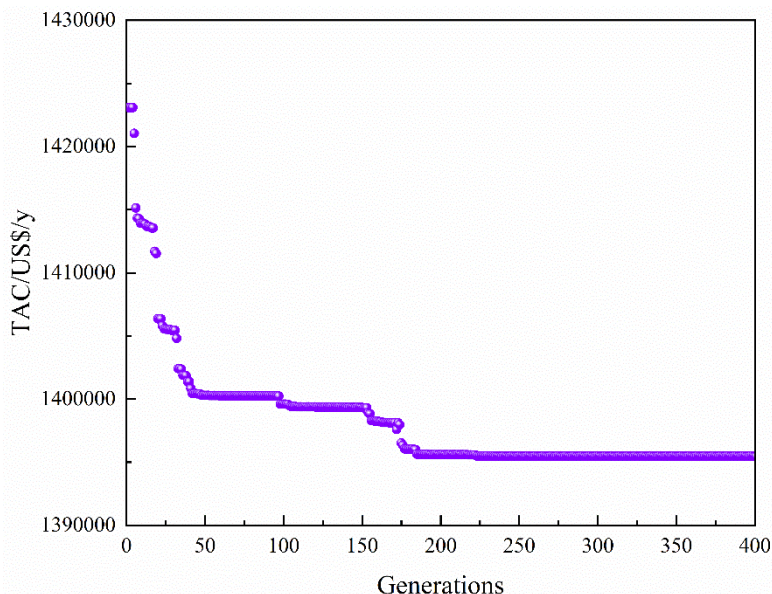
239 In the indirect process, it is necessary to separate the THF-EtAC mixture. Figure S2 gives T-xy diagram for  
 240 THF-EtAC under 1.0 and 0.5 bar. As illustrated in Fig. S2a, the high purity of THF could not be obtained at 1.0  
 241 bar because the vapor and liquid lines are extremely close to each other (see the blue circle). The corresponding  
 242 T-xy diagram of this binary system under 0.5 bar is shown in Fig. S2b. As indicated, to use such a reduced  
 243 pressure makes this binary separation possible [50]. For the EDCs in both direct and indirect processes, we chose  
 244 to operate them at 0.5 bar as well because this can increase the relative volatility of both EtAC-water and THF-  
 245 water systems (see the uni-volatility lines at 1.0 bar and 0.5 bar in Figure S3). To use an even lower pressure will  
 246 dramatically increase the cost for vacuuming thus is not considered here. For the ERC in both direct and indirect  
 247 processes, the task is to separate water and DMSO. We plot the x-y diagram for this binary system in Figure S4.  
 248 As demonstrated, this binary mixture is easy to separate regardless of the operating pressure. Herein, 0.5 bar is  
 249 selected again because keeping the same pressure level as the previous columns can save pumping cost. Moreover,  
 250 a reduced operating pressure in the ERC is also beneficial for decreasing the reboiler temperature, which helps  
 251 save the cost for high-pressure steam. In summary, all the distillation columns are operated at 0.5 bar.

### 252 3.3 Process optimization results

253 The optimization of the two proposed processes is implemented in the desktop computer with Intel® Core™ i7-  
 254 7700 CPU@3.60 GHZ and 8G RAM. Table S5 summarizes the setup parameters of the improved GA used in the  
 255 optimization process as suggested by our previous work [41].

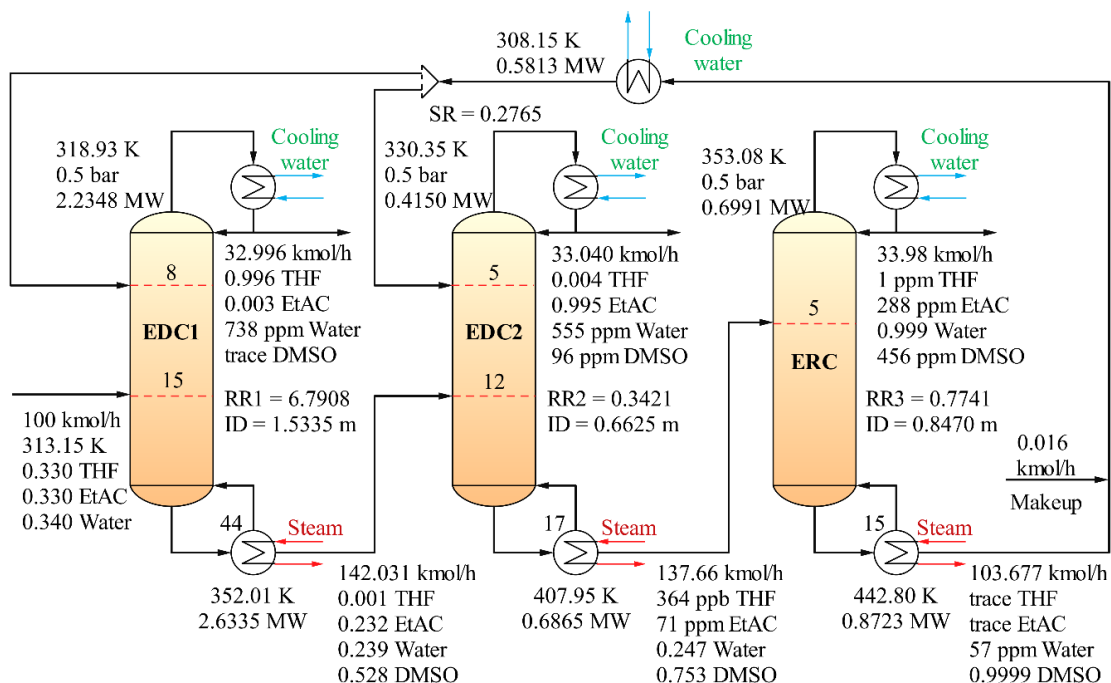
#### 256 3.3.1 Direct TCED process

257 Fig. 6 illustrates the dependence of the TAC of the direct TCED process on the number of generations. The  
 258 optimization is stopped at 400 generations because the tolerance is lower than  $10^{-5}$ . The whole process takes 1108  
 259 minutes. The optimal direct TCED process for separating the ternary azeotropic mixture THF/EtAC/water is  
 260 demonstrated in Fig. 7 where all the stream information and column specifications are provided.



261  
262

**Fig. 6** The optimization result of the direct TCED process



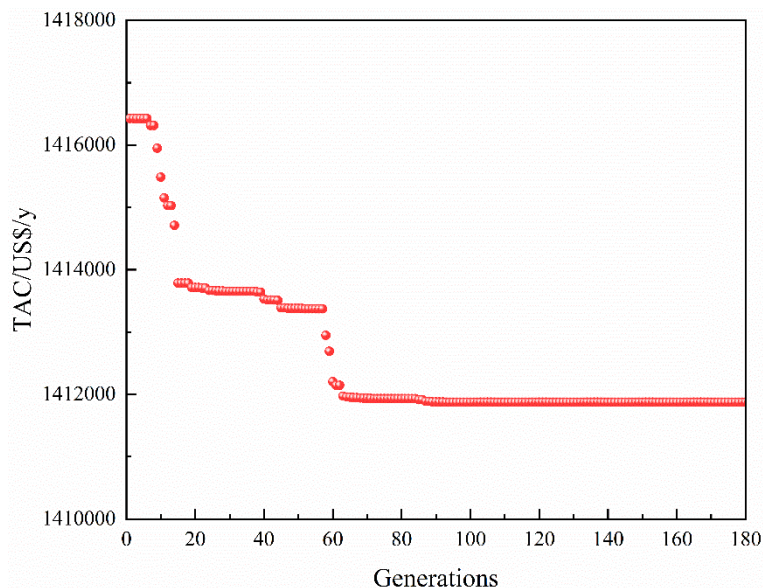
263  
264

**Fig. 7** The optimal direct TCED process for separating THF/EtAC/water using DMSO as the entrainer

265 Fig. S5 shows the liquid composition and temperature profiles of the optimal direct separation process. As  
266 demonstrated, THF, EtAC and water with high-purities are respectively distilled at the top of EDC1, EDC2 and  
267 ERC (Stage 1 of Fig. S5 a, c, and e). The DMSO with 99.99 mol% is obtained at the bottom of ERC. Moreover,  
268 temperature transitions can be observed near (or at) the feed locations, as shown in Fig. S5 b, d, and f.

### 269 3.3.2 Indirect TCED process

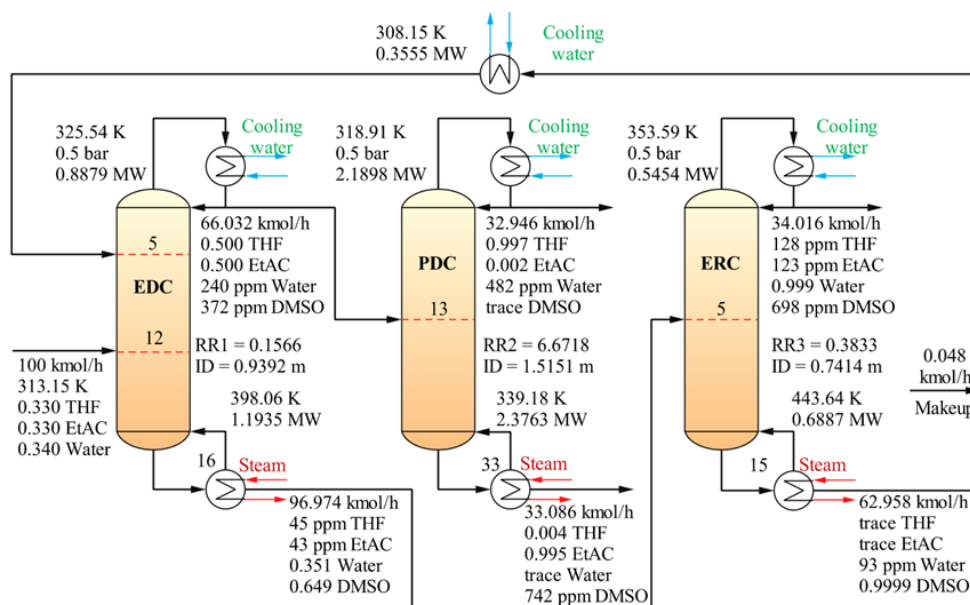
270 The reduction of TAC with number of generations for the indirect TCED process is given in Fig. 8. As shown,  
271 the optimization is terminated at 180 generations when the tolerance is lower than  $10^{-5}$ . The whole calculation  
272 takes about 602 minutes.



273

274 **Fig. 8** The optimization results of the indirect TCED process

275 Fig. 9 illustrates the optimal indirect TCED process for separating the ternary azeotropic mixture  
 276 THF/EtAC/water. The total number of stages of EDC, PDC and ERC are 16, 33 and 15, respectively. The  
 277 entrainer DMSO and the ternary mixture are fed into the 5<sup>th</sup> and 12<sup>th</sup> trays of EDC while the feed locations of  
 278 PDC and ERC are the 13<sup>th</sup> and 5<sup>th</sup> stages, respectively. To achieve the separation of THF/EtAC and water, 63.006  
 279 kmol/h of DMSO and 0.1566 of reflux ratio are required in the EDC. High purities of THF and EtAC (*i.e.*, 99.7  
 280 mol% and 99.5 mol%) are obtained at the top and bottom of PDC. Water and DMSO are finally separated in the  
 281 ERC column with 0.3833 of reflux ratio. The condenser duties of the three columns are 0.8879 MW, 2.1898MW,  
 282 and 0.5454 MW while the corresponding reboiler duties are 1.1935 MW, 2.3763 MW, and 0.6887 MW,  
 283 respectively.



284

285 **Fig. 9** The optimal indirect TCED process for separating THF/EtAC/water using DMSO as the entrainer

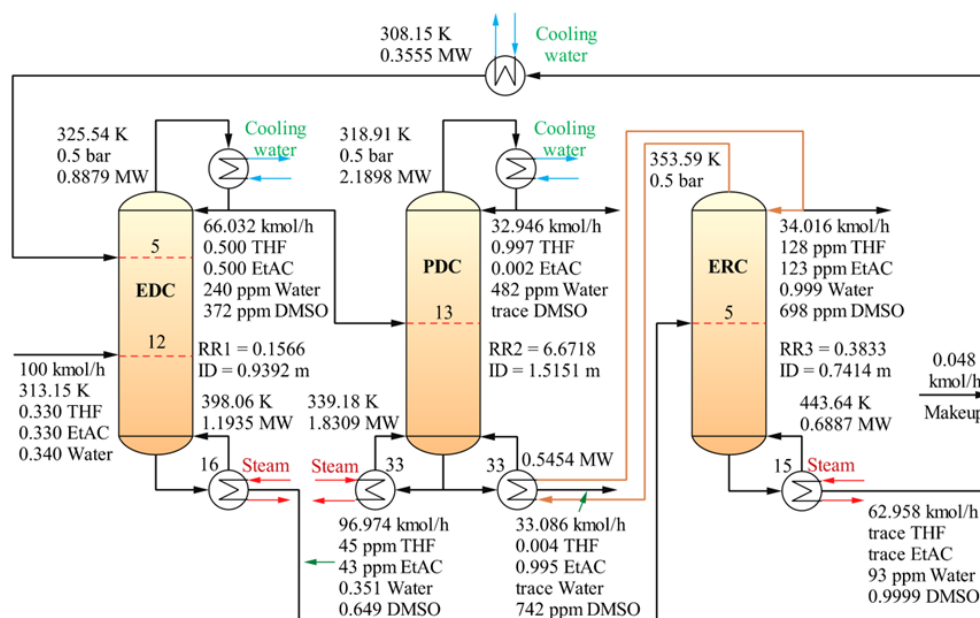
286 The liquid composition and temperature profiles of the indirect TCED process are displayed in Fig. S6. As  
 287 indicated, THF/EtAC and water are separated at the extractive section (from 5<sup>th</sup> to 12<sup>th</sup> tray) while the  
 288 concentrations of THF and EtAC get accumulated towards the top of the ED column. Notably, remixing occurs

289 in the stripping section, resulting in more heat input. The composition and temperature profiles in PDC and ERC  
 290 are easy to interpret because both of the columns separate binary mixtures.

### 291 3.4 HI results

292 As illustrated in Fig. 7, the HI technology could not be employed for the direct TCED process because the  
 293 difference between the temperature in the condenser (353.08 K) and the temperature in the reboiler (352.01 K)  
 294 is too small. However, HI can be adopted to further reduce the energy consumption of the indirect TCED process  
 295 because the temperature difference between the top of ERC and the bottom of PDC is higher than 14 K, as  
 296 illustrated in Fig. 9.

297 Fig. 10 depicts the optimal indirect TCED process where HI is applied. As shown, the reboiler duty of the  
 298 PDC can be divided into two parts with 0.5454 MW supplied by the top vapor stream of the ERC and 1.8309  
 299 MW provided by external steam. In other words, we can save 0.5454 MW heating and cooling duties by  
 300 employing HI.



301  
 302 **Fig. 10** The optimal indirect TCED process with HI scheme for separating THF/EtAC/water using DMSO as the entrainer

### 303 3.5 Comparison and discussions

304 The economic performance for the direct and indirect processes without and with HI is summarized in Table 2.  
 305 The TAC of the three processes are 1,397,320.33 US\$/y, 1,413,626.41 US\$/y and 1,373,366.41 US\$/y,  
 306 respectively. As indicated, the proposed direct process with 99.6 mol% THF purity shows a higher performance  
 307 than the indirect one because it can avoid the repeat heating of components. Of note is that, a relatively higher  
 308 THF purity (99.7 mol%) and economic performance could be achieved via the indirect TCED process after HI is  
 309 employed.

310 **Table 2.** Economic performance of the direct and indirect processes with and without HI

	Direct process	Indirect process without HI	Indirect process with HI
TCC (US\$)	1,219,334.38	1,229,563.80	1,141,299.66
AOC (US\$/y)	990,875.54	1,003,771.81	992,933.19

	Direct process	Indirect process without HI	Indirect process with HI
TAC (US\$/y)	1,397,320.33	1,413,626.41	1,373,366.41

## 311 4 Conclusion

312 In this contribution, an energy-efficient TCED process is developed for recovering THF and EtAC from industrial  
313 wastewater. A rigorous hierarchical design procedure involving entrainer design, thermodynamic analysis,  
314 process design and optimization, and HI is followed in the process development. First, candidate entrainers are  
315 screened via the CAMD method, and then the most efficient entrainer DMSO is determined via the comparison  
316 of the iso- and uni- volatility lines. Later, two alternatives of direct and indirect TCED processes are proposed.  
317 An improved GA is employed to optimize the proposed two processes. HI is finally performed for the optimized  
318 processes. The TAC of the direct TCED process, indirect process without and with HI are 1,397,320.33 US\$/y,  
319 1,413,626.41 US\$/y, and 1,373,366.41 US\$/y, respectively, which proves that the indirect separation process with  
320 HI is the best process alternative for separating THF/EtAC/water.

321 In order to reduce the remixing effects of the direct and indirect processes, intensified configurations such  
322 as dividing wall column and side-stream ED will be explored in the future work. In addition, innovative solvents  
323 such as ionic liquids will be considered in the entrainer design to find a potentially better ED process. Finally,  
324 life cycle environmental assessment can be included in the optimal process design.

325 **Acknowledgment** This work is financially supported by the National Key Research and Development Project  
326 (2019YFC0214403), the Joint Supervision Scheme with the Chinese Mainland, Taiwan and Macao Universities  
327 - Other Chinese Mainland, Taiwan and Macao Universities (Grant No. SB2S to Yang A), and the Research  
328 Committee of The Hong Kong Polytechnic University for the financial support of the project through a PhD  
329 studentship (Project account code RK3P to Shi T).

330 **Electronic Supplementary Material** Supplementary material is available in the online version of this article  
331 at [http://dx.doi.org/\[DOI\]](http://dx.doi.org/[DOI]) and is accessible for authorized users.

## 332 References

- 333 1. Santaella M A, Orjuela A, Narváez P C. Comparison of different reactive distillation schemes for ethyl acetate production using  
334 sustainability indicators. *Chemical Engineering and Processing: Process Intensification*, 2015, 96: 1-13
- 335 2. Tran L S, Verdicchio M, Monge F, Martin R C, Bounaceur R, Sirjean B, Glaude P A, Alzueta M U, Battin-Leclerc F. An  
336 experimental and modeling study of the combustion of tetrahydrofuran. *Combustion and Flame*, 2015, 162(5): 1899-1918
- 337 3. He Z, Lin S, Gong C, Xi Y. Study on separating tetrahydrofuran from the mixture made up tetrahydrofuran, ethyl acetate and  
338 water. *Journal of Shenyang Institute of Chemical Technology*, 1996, 10(2): 143-147
- 339 4. Deorukhkar O A, Deogharkar B S, Mahajan Y S. Purification of tetrahydrofuran from its aqueous azeotrope by extractive  
340 distillation: Pilot plant studies. *Chemical Engineering and Processing: Process Intensification*, 2016, 105: 79-91
- 341 5. Yin Y, Yang Y, de Lourdes Mendoza M, Zhai S, Feng W, Wang Y, Gu M, Cai L, Zhang L. Progressive freezing and suspension  
342 crystallization methods for tetrahydrofuran recovery from Grignard reagent wastewater. *Journal of Cleaner Production*, 2017, 144: 180-186
- 343 6. Zhang X, He J, Cui C, Sun J. A systematic process synthesis method towards sustainable extractive distillation processes with  
344 pre-concentration for separating the binary minimum azeotropes. *Chemical Engineering Science*, 2020, 227: 115932
- 345 7. Gracová E, Šulgan B, Barabas S, Steltenpohl P. Methyl acetate–methanol mixture separation by extractive distillation:  
346 Economic aspects. *Frontiers of Chemical Science and Engineering*, 2018, 12(4): 670-682
- 347 8. Wang C, Zhang Z, Zhang X, Guang C, Gao J. Comparison of pressure-swing distillation with or without crossing curved-  
348 boundary for separating a multiazeotropic ternary mixture. *Separation and Purification Technology*, 2019, 220: 114-125
- 349 9. Liang S, Cao Y, Liu X, Li X, Zhao Y, Wang Y, Wang Y. Insight into pressure-swing distillation from azeotropic phenomenon to  
350 dynamic control. *Chemical Engineering Research and Design*, 2017, 117: 318-335
- 351 10. Han Z, Ren Y, Li H, Li X, Gao X. Simultaneous extractive and azeotropic distillation separation process for production of poden  
352 from formaldehyde and methylal. *Industrial & Engineering Chemistry Research*, 2019, 58(13): 5252–5260

- 353 11. Haaz E, Szilagyı B, Fozer D, Toth A J. Combining extractive heterogeneous-azeotropic distillation and hydrophilic pervaporation  
354 for enhanced separation of non-ideal ternary mixtures. *Frontiers of Chemical Science and Engineering*, 2020, 14(5): 913-927
- 355 12. Yang A, Shen W, Wei S, Dong L, Li J, Gerbaud V. Design and control of pressure-swing distillation for separating ternary systems  
356 with three binary minimum azeotropes. *AIChE Journal*, 2019, 65(4): 1281-1293
- 357 13. Li W, Zhong L, He Y, Meng J, Yao F, Guo Y, Xu C. Multiple steady-states analysis and unstable operating point stabilization in  
358 homogeneous azeotropic distillation with intermediate entrainer. *Industrial & Engineering Chemistry Research*, 2015, 54(31): 7668-7686
- 359 14. Gerbaud V, Rodriguez-Donis I, Hegely L, Lang P, Denes F, You X. Review of extractive distillation. Process design, operation,  
360 optimization and control. *Chemical Engineering Research and Design*, 2019, 141: 229-271
- 361 15. Li H, Wu Y, Li X, Gao X. State-of-the-art of advanced distillation technologies in China. *Chemical Engineering & Technology*,  
362 2016, 39(5): 815-833
- 363 16. Yang A, Sun S, Shi T, Xu D, Ren J, Shen W. Energy-efficient extractive pressure-swing distillation for separating binary minimum  
364 azeotropic mixture dimethyl carbonate and ethanol. *Separation and Purification Technology*, 2019, 229: 115817
- 365 17. Shi T, Yang A, Jin S, Shen W, Wei S, Ren J. Comparative optimal design and control of two alternative approaches for separating  
366 heterogeneous mixtures isopropyl alcohol-isopropyl acetate-water with four azeotropes. *Separation and Purification Technology*, 2019, 225:  
367 1-17
- 368 18. Pan Q, Shang X, Li J, Ma S, Li L, Sun L. Energy-efficient separation process and control scheme for extractive distillation of  
369 ethanol-water using deep eutectic solvent. *Separation and Purification Technology*, 2019, 219: 113-126
- 370 19. Shi X, Zhu X, Zhao X, Zhang Z. Performance evaluation of different extractive distillation processes for separating ethanol/tert-  
371 butanol/water mixture. *Process Safety and Environmental Protection*, 2020, 137: 246-260
- 372 20. Yang A, Zou H, Chien I L, Wang D, Wei S, Ren J, Shen W. Optimal design and effective control of triple-column extractive  
373 distillation for separating ethyl acetate/ethanol/water with multiazeotrope. *Industrial & Engineering Chemistry Research*, 2019, 58(17):  
374 7265-7283
- 375 21. Cignitti S, Rodriguez-Donis I, Abildskov J, You X, Shcherbakova N, Gerbaud V. CAMD for entrainer screening of extractive  
376 distillation process based on new thermodynamic criteria. *Chemical Engineering Research and Design*, 2019, 147: 721-733
- 377 22. Woo H C, Kim Y H. Solvent selection for extractive distillation using molecular simulation. *AIChE Journal*, 2019, 65(9): e16665
- 378 23. Cui Y, Zhang Z, Shi X, Guang C, Gao J. Triple-column side-stream extractive distillation optimization via simulated annealing  
379 for the benzene/isopropanol/water separation. *Separation and Purification Technology*, 2020, 236: 116303
- 380 24. Zhu Z, Li G, Dai Y, Cui P, Xu D, Wang Y. Determination of a suitable index for a solvent via two-column extractive distillation  
381 using a heuristic method. *Frontiers of Chemical Science and Engineering*, 2020, 14(5): 824-833
- 382 25. Shen W, Dong L, Wei S, Li J, Benyounes H, You X, Gerbaud V. Systematic design of an extractive distillation for maximum-  
383 boiling azeotropes with heavy entrainers. *AIChE Journal*, 2015, 61(11): 3898-3910
- 384 26. Blahuřiak M, Kiss A A, Babic K, Kersten S R A, Bargeman G, Schuur B. Insights into the selection and design of fluid separation  
385 processes. *Separation and Purification Technology*, 2018, 194: 301-318
- 386 27. Gani R, Brignole E. Molecular design of solvents for liquid extraction based on UNIFAC. *Fluid Phase Equilibria*, 1983, 13: 331-  
387 340
- 388 28. Gertig C, Kröger L, Fleitmann L, Scheffczyk J, Bardow A, Leonhard K. Rx-COSMO-CAMD: Computer-aided molecular design  
389 of reaction solvents based on predictive kinetics from quantum chemistry. *Industrial & Engineering Chemistry Research*, 2019, 58(51):  
390 22835-22846
- 391 29. Liu Q, Zhang L, Liu L, Du J, Meng Q, Gani R. Computer-aided reaction solvent design based on transition state theory and  
392 COSMO-SAC. *Chemical Engineering Science*, 2019, 202: 300-317
- 393 30. Zhou T, Wang J, McBride K, Sundmacher K. Optimal design of solvents for extractive reaction processes. *AIChE Journal*, 2016,  
394 62(9): 3238-3249
- 395 31. Zhang L, Pang J, Zhuang Y, Liu L, Du J, Yuan Z. Integrated solvent-process design methodology based on COSMO-SAC and  
396 quantum mechanics for TMQ (2,2,4-trimethyl-1,2-H-dihydroquinoline) production. *Chemical Engineering Science*, 2020, 226: 115894
- 397 32. Song Z, Zhang C, Qi Z, Zhou T, Sundmacher K. Computer-aided design of ionic liquids as solvents for extractive desulfurization.  
398 *AIChE Journal*, 2018, 64(3): 1013-1025
- 399 33. Chao H, Song Z, Cheng H, Chen L, Qi Z. Computer-aided design and process evaluation of ionic liquids for n-hexane-  
400 methylcyclopentane extractive distillation. *Separation and Purification Technology*, 2018, 196: 157-165
- 401 34. Zhou T, Song Z, Zhang X, Gani R, Sundmacher K. Optimal solvent design for extractive distillation processes: A multiobjective  
402 optimization-based hierarchical framework. *Industrial & Engineering Chemistry Research*, 2019, 58(15): 5777-5786



- 403 35. Silva R O, Torres C M, Bonfim-Rocha L, Lima O C M, Coutu A, Jiménez L, Jorge L M M. Multi-objective optimization of an  
404 industrial ethanol distillation system for vinasse reduction-A case study. *Journal of Cleaner Production*, 2018, 183: 956-963
- 405 36. Waltermann T, Grueters T, Muenchrath D, Skiborowski M. Efficient optimization-based design of energy-integrated azeotropic  
406 distillation processes. *Computers & Chemical Engineering*, 2020, 133: 106676
- 407 37. Krone D, Esche E, Asprion N, Skiborowski M, Repke J U, Conceptual design based on superstructure optimization in GAMS  
408 with accurate thermodynamic models. *Computer Aided Process Engineering*, 2020, 48: 15-20
- 409 38. Li X, Cui C, Li H, Gao X. Process synthesis and simulation-based optimization of ethylbenzene/styrene separation using double-  
410 effect heat integration and self-heat recuperation technology: A techno-economic analysis. *Separation and Purification Technology*, 2019,  
411 228: 115760
- 412 39. Su Y, Jin S, Zhang X, Shen W, Eden M R, Ren J. Stakeholder-oriented multi-objective process optimization based on an improved  
413 genetic algorithm. *Computers & Chemical Engineering*, 2020, 132: 106618
- 414 40. Kruber K F, Grueters T, Skiborowski M, Efficient design of intensified extractive distillation processes based on a hybrid  
415 optimization approach. *Computer Aided Process Engineering*, 2019, 46: 859-864
- 416 41. Yang A, Su Y, Chien I L, Jin S, Yan C, Wei S, Shen W. Investigation of an energy-saving double-thermally coupled extractive  
417 distillation for separating ternary system benzene/toluene/cyclohexane. *Energy*, 2019, 186: 115756
- 418 42. You X, Gu J, Gerbaud V, Peng C, Liu H. Optimization of pre-concentration, entrainer recycle and pressure selection for the  
419 extractive distillation of acetonitrile-water with ethylene glycol. *Chemical Engineering Science*, 2018, 177: 354-368
- 420 43. Momoh S O. Assessing the accuracy of selectivity as a basis for solvent screening in extractive distillation processes. *Separation  
421 Science and Technology*, 1991, 26(5): 729-742
- 422 44. Marrero J, Gani R. Group-contribution based estimation of pure component properties. *Fluid Phase Equilibria*, 2001, 183: 183-  
423 208
- 424 45. Rodriguez-Donis I, Gerbaud V, Joulia X. Thermodynamic insights on the feasibility of homogeneous batch extractive distillation,  
425 1. azeotropic mixtures with a heavy entrainer. *Industrial & Engineering Chemistry Research*, 2009, 48(7): 3544-3559
- 426 46. Douglas J M. *Conceptual design of chemical processes*. 1st ed. New York: McGraw-Hill, 1988, 461-462
- 427 47. Luyben W L. *Distillation design and control using Aspen simulation*. 1st ed. New Jersey: John Wiley & Sons, 2013, 87-89
- 428 48. Zhang Q, Liu M, Li C, Zeng A. Heat-integrated pressure-swing distillation process for separation of the maximum-boiling  
429 azeotrope diethylamine and methanol. *Journal of the Taiwan Institute of Chemical Engineers*, 2018, 93: 644-659
- 430 49. Yang J, Pan X, Yu M, Cui P, Ma Y, Wang Y, Gao J. Vapor-liquid equilibrium for binary and ternary systems of tetrahydrofuran,  
431 ethyl acetate and N-methyl pyrrolidone at pressure 101.3 kPa. *Journal of Molecular Liquids*, 2018, 268: 19-25
- 432 50. Xia M, Shi H, Niu C, Ma Z, Lu H, Xiao Y, Hou B, Jia L, Li D. The importance of pressure-sensitive pinch/azeotrope feature on  
433 economic distillation design. *Separation and Purification Technology*, 2020, 250: 116753